URSI AP-RASC, Sydney, Australia, 17 – 22 August 2025

GNSS-based Ionospheric Observations after the Noto Peninsula Earthquake and Tsunami

F. Luhrmann(1), J. Park (1)
(1) Oregon State University, Corvallis, OR, 97331, https://engineering.oregonstate.edu/

Abstract

On 1 January 2024 a M7.5 earthquake struck the Noto Peninsula of Japan at 2024-01-01 07:10:09 (UTC). We use ground-based Global Navigation Satellite Systems (GNSS) data from GEONET (GNSS Earth Observation Network System) receivers operated by the Geospatial Information Authority of Japan (GSI) and the Continuously Operating Reference Station (CORS) operated by the National Geographic Information Institute (NGII) in South Korea to analyze the ionospheric response to this earthquake and resulting tsunami event. An N-shaped co-seismic ionospheric disturbance is observed in the total electron content (TEC) measurements between eight to fifteen minutes after the earthquake across 91 GSI's GEONET stations and 11 satellites. We observed a variety of co-seismic ionospheric disturbance velocities and directions while the event is relatively smaller than other major submarine earthquakes with a depth of 10km. The predominant co-seismic ionospheric disturbances (CSID) propagated from the epicentral area with a velocity of 800 m/s, extending 650 km from the epicenter. A secondary disturbance potentially due to the tsunami is under investigation.

1. Introduction

Major ground explosions and large earthquakes generate acoustic pressure waves that propagate vertically and displace the electron density profile of the ionosphere, the upper region of earth's atmosphere [1]. Displacements due to earthquake events are described as co-seismic ionospheric disturbances (CSID) and are observable in total electron content (TEC) measurements made by ground-based Global Navigation Satellite Systems (GNSS) receivers [2]. The observations by GNSS TEC measurements show the initial disturbance from an acoustic wave to emerge ten minutes after the earthquake event on average and propagate at an approximate velocity of 800 m/s [3].

In addition to CSID, ionospheric disturbances have also been detected as a result of tsunami events that generate internal gravity waves (IGWs) [4]. These ionospheric disturbances travel at a velocity between 200 to 220 m/s with smaller amplitudes of 0.1 - 0.2 TEC Units, 10^16 electrons/m² [5]. A tsunami induced ionospheric disturbance resulting from an earthquake event can be observable 500 km from the epicentral area between 25 to 60 minutes after the earthquake event [5]. These distance, velocity, and timing metrics help distinguish tsunami signatures from earthquake signatures when the events are co-occurring.

A M7.5 earthquake struck the Noto Peninsula of Japan on 1 January 2024, with a reported epicenter of 37.487ºN, 137.271ºE at a depth of 10 km (USGS). The earthquake occurred as a result of shallow reverse faulting in the northeast-southwest striking planes. Observed displacement analysis from the GEONET stations shows the largest vertical uplift to the southwest of the reported epicenter and horizontal displacement to the western direction [6]. A foreshock was observed with M5.5 four minutes before and an aftershock of M6.2 nine minutes after the earthquake event [7]. Aftershocks were recorded along the peninsula and adjacent offshore areas with an extent of 150 km [6]. A tsunami was generated by the earthquake and tsunami waves were observed across wave and tide gauges along the west coast of Japan and the east coast of South Korea. The earliest waves arrived at Suzu city, one minute after the earthquake event, reaching heights over 4.7m [7]. The earthquake and resulting tsunami caused extensive damage, flooding along the west coast of Japan, and sadly over 200 deaths.

Using ground-based GNSS receiver measurements of ionospheric TEC across Japan and Korea, we detect CSID approximately 9 minutes after the Noto peninsula earthquake with a predominate velocity of 800 m/s within the range of ±0.5 TECU. The acoustic wave disturbances were primarily to the east of the epicentral area; minor disturbances are visible to the west as shown in Figure 2. Disturbances extended 650 km from the earthquake epicentral area.

2. Preliminary Results

To study the ionospheric signatures driven by the earthquake and resulting tsunami we used 238 GSI GEONET data at 30 second sample rate and 10 NGII CORS data at both 30 second and 1 second sample rates for this report. The 238 GEONET receivers were selected within a 200 km area from the epicentral region. TEC Line-of-sight (LOS) measurements are estimated with the linear combination of dual-frequency L1 and L2 measurements as seen in [8]. These values are processed with a fourth-order Butterworth high-pass filter, removing frequencies below 1 mHz.

Preliminary results show an ionospheric disturbance as a result of the earthquake generated acoustic wave with a velocity of 800 m/s primarily east of the epicenter area, Figures 1, 2, and 5. In Figure 1, there is evidence of a secondary disturbance in several of the signals, potentially a result from the M6.2 aftershock event. This requires further analysis to confirm. A potential IGW disturbance due to the resulting tsunami is evident by the 200 m/s velocity wave shown in Figure 5, but will require further analysis to confirm the ionospheric pierce point (IPP) of its location. Signals that have a high potential of capturing a tsunami disturbance are shown in Figure 3 with their corresponding IPP shown in Figure 4.

5. Figures

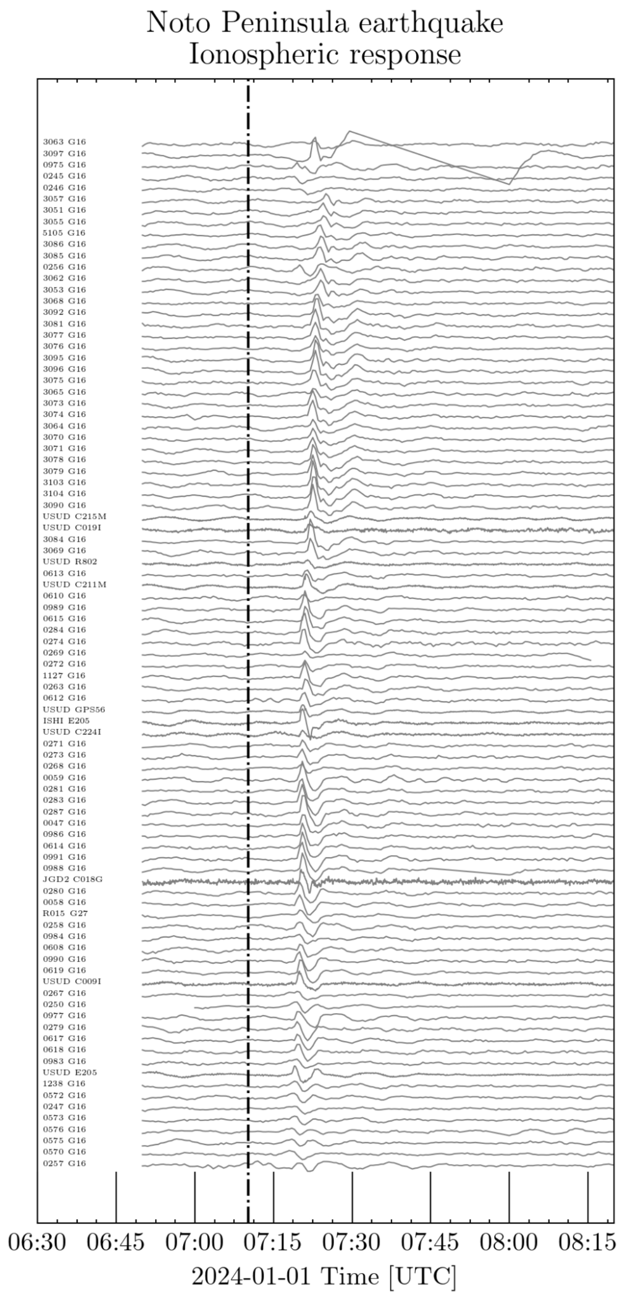

Figure 1. TEC calculated across Japan GNSS stations plotted from bottom to top by max TECU after the M7.5 earthquake at 07:10:09 UTC, indicated by the vertical dashed line. Station name and Satellite are listed along the right of the plot. The IPP locations of these signals are shown in Figure 2.

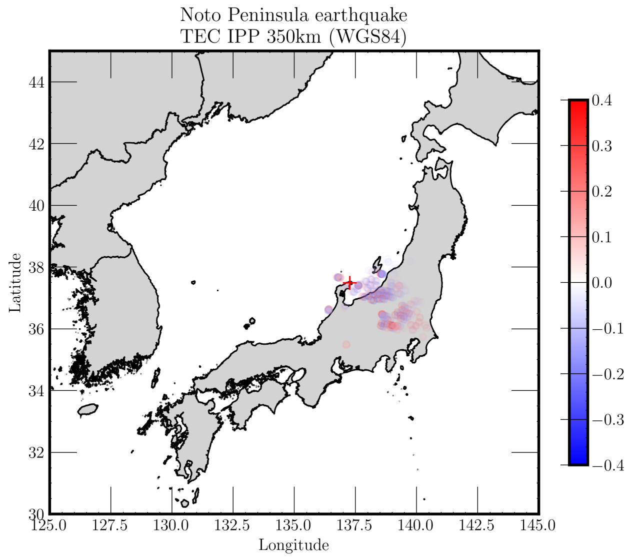

Figure 2. The location of the TEC measurements in Figure 1 are shown around the epicentral area, shown with the red cross, at the Noto Peninsula. A majority of the disturbances are observed to the east of the epicentral area.

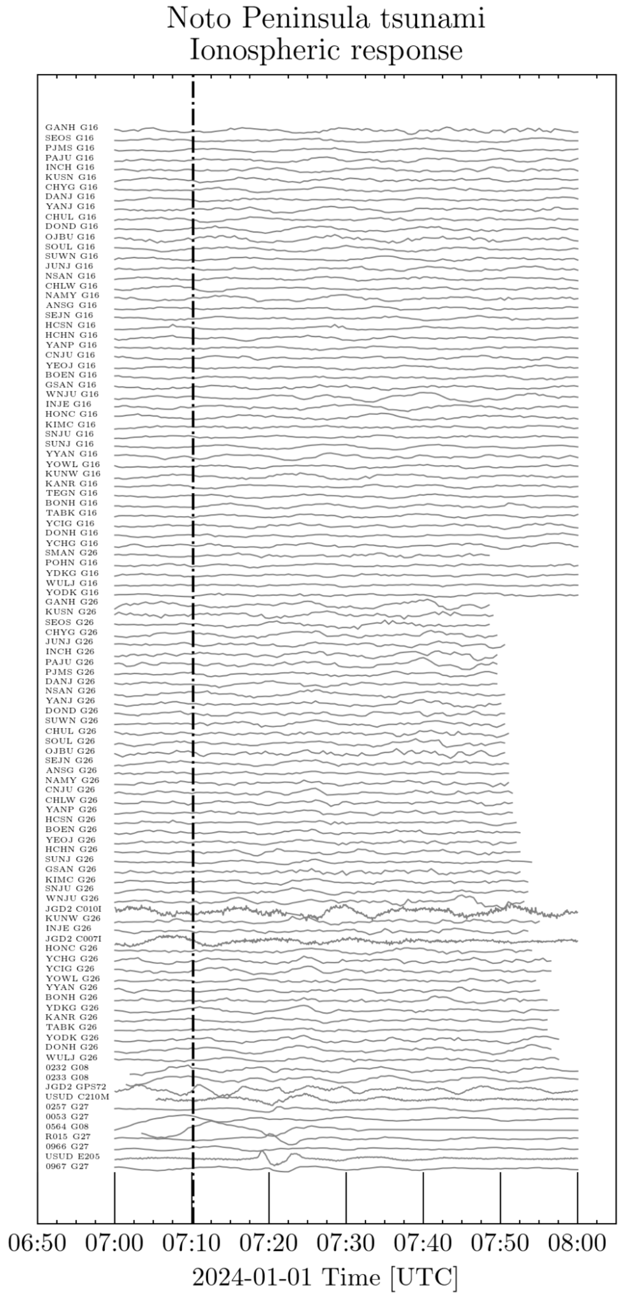

Figure 3. These are the station and satellite TEC observations whose line of sight covers the Sea of Japan after the 2024-01-01 earthquake on the Noto Peninsula, Japan. Plotted from bottom to top by distance to the M7.5 earthquake at 07:10:09 UTC, indicated by the vertical dashed line. The IPP locations of these signals are shown in Figure 4.

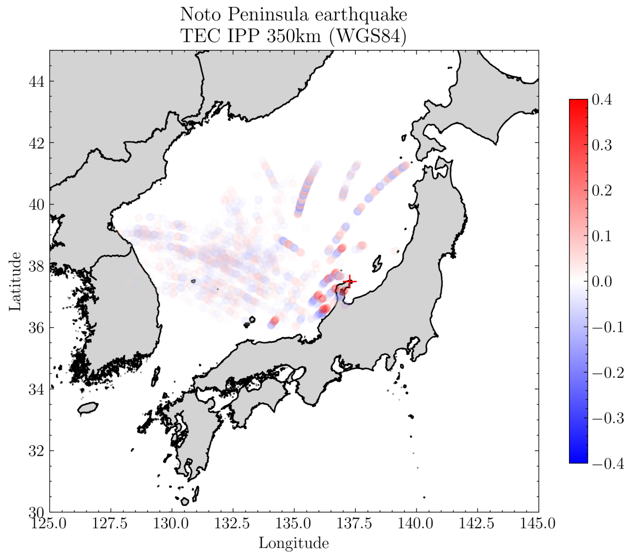

Figure 4. The location of the TEC measurements in Figure 4 are shown around the epicentral area, shown with the red cross, at the Noto Peninsula.

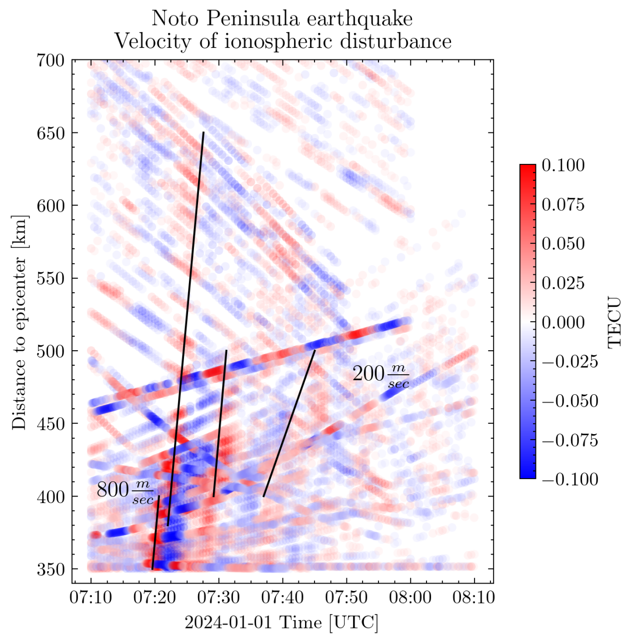

Figure 5. A primary ionospheric disturbance velocity of 800 m/s is shown above by plotting the TECU values, with distance to the earthquake epicenter on the Y-axis, and Time on the X-axis. The ionospheric oscillation of the electron density due to the acoustic wave, as measured by TECU, is shown by the change between red to blue over time. A potential IGW caused by the tsunami is called out with the 200m/s sloped black line.

References

[1] N. Y. Kotsarenko, R. P. rez Enr quez, and S.V. Koshevaya. Excitation of plasma waves in the ionosphere caused by atmospheric acoustic waves.

Astrophysics and Space Science, **246**, 2, 1996 pp. 211–217, doi:10.1007/BF00645641

[2] E. Calais and J. B. Minster. GPS detection of ionospheric perturbations following the January 17, 1994, Northridge Earthquake. *Geophysical Research Letters*, **22**, 9, 1995, pp. 1045–1048. doi:10.1029/95GL00168

[3] K. Heki, M. S. Bagiya, and Y. Takasaka. Slow fault slip signatures in coseismic ionospheric disturbances. *Geophysical Research Letters*, **49**, 24, 2022, doi:10.1029/2022GL101064

[4] G. Occhipinti, L. Rolland, P. Lognonne, and S. Watada. From Sumatra 2004 to Tohoku-Oki 2011; the systematic GPS detection of the ionospheric signature induced by tsunamigenic earthquakes. *Journal of Geophysical Research. Space Physics*, **118**, 6, 2013, pp. 3626–3636. doi: 10.1002/jgra.50322

[5] D. A. Galvan, A. Komjathy, Y. T. Song, P. Stephens, M. P. Hickey, and J. Foster. Observing Tsunamis in the Ionosphere Using Ground Based GPS Measurements. 2011, Jet Propulsion Laboratory.

[6] Y. Fujii, and K. Satake. Slip distribution of the 2024 Noto Peninsula earthquake. *Earth, Planets, and Space*, **76**, 1, 2024, doi:10.1186/s40623-024-01991-z

[7] K. Pakoksung, A. Suppasri, and F. Imamura. Preliminary modeling and analysis of the Tsunami generated by the 2024 Noto Peninsula earthquake on 1 January: Wave characteristics in the Sea of Japan. *Ocean Engineering*, 307, 2024, 118172-. doi:10.1016/j.oceaneng.2024.118172

[8] P. Teunissen, O. Montenbruck, and P. J. G. Teunissen. Springer Handbook of Global Navigation Satellite Systems (1st ed.). Springer International Publishing AG. 2017, doi:10.1007/978-3-319-42928-1